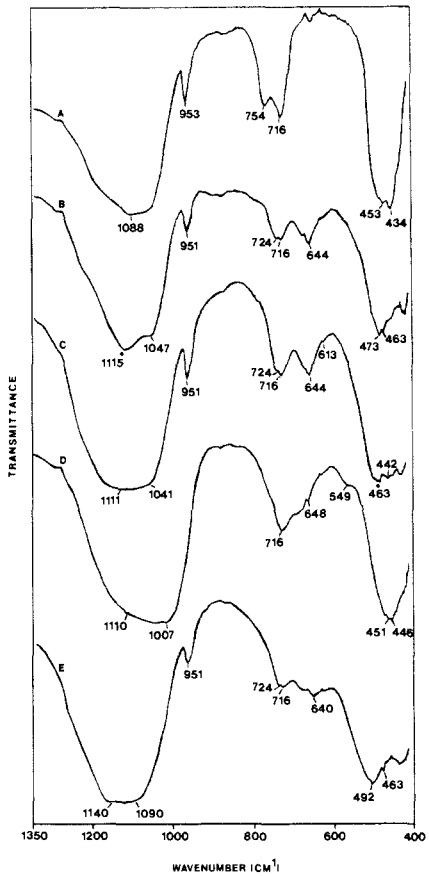

Figure 10. Infrared spectra of the structural region for molecular sieves: (A) sodalite, (B) SAPO-20A, (C) SAPO-20B, (D) SAPO-20C, (E) $AlPO_4$-20.

Infrared Results. Figure 10 shows the infrared spectra of the structural region for the five molecular sieves with the sodalite structure. The infrared spectrum of TMA–sodalite is illustrated by A. The peak at 953 cm^{-1} is from TMA^+. Flanigen et al.[33] show the infrared spectrum for hydroxy sodalite. In general spectrum A agrees with that of Flanigen et al. except that the absorptions between 700 and 760 cm^{-1} are at higher wavenumber (754 and 716 cm^{-1} compared to 729 and 660 cm^{-1}). The broad band around 1000–1100 cm^{-1} has been assigned to the asymmetric stretching of tetrahedra[33] and is characteristic of zeolite materials. Notice that, for SAPO-20A, SAPO-20B, and $AlPO_4$-20, this region is shifted to higher wavenumber. The shift is due to the presence of large amounts of phosphorus since the P–O bond distance is shorter than either Si–O or Al–O. SAPO-20C shows a very broad absorption in this region as might be expected since the solid contains some phosphorus but still possesses a Si/Al of a zeolite. In the region of 750 cm^{-1} and below, there are many differences in the number and frequency of the absorptions for the five materials reflecting the variation in framework composition.

Finally, upon calcination of SAPO-20A, SAPO-20B, and SAPO-20C, hydroxyl group absorptions are observed for each material. Thus, at least a portion of the TMA in all three samples is compensating framework charge.

Conclusions

The overall results of this study and our previous work[10] lead to the following conclusions. The atomic arrangements of Al, Si, and P in molecular sieves are such that Si–O–P linkages are not observed. Thus, in terms of substitution mechanisms, Si^{4+} can substitute for P^{5+} and vice versa, and Si–O–Si can substitute for Al–O–P and vice versa.

Acknowledgment. Financial support of this work was provided by the National Science Foundation under the Presidential Young Investigator Award to M.E.D. and The Dow Chemical Co. We thank Dr. Steven Suib, Chemistry Department, University of Connecticut, for the XPS analysis of SAPO-37.

Registry No. (TPA)OH, 4499-86-9; (TMA)OH, 75-59-2; $(TMA)^+$, 51-92-3; Cab-O-Sil, 7631-86-9; H_3PO_4, 7664-38-2; Al(O)(OH), 24623-77-6.

(33) Flanigen, E. M.; Khatami, H.; Szymanski, H. A. *Molecular Sieve Zeolites-I*; American Chemical Society: Washington, DC 1971; p 201–228.

The System Pyridine–Hydrogen Fluoride at Low Temperatures: Formation and Crystal Structures of Solid Complexes with Very Strong NHF and FHF Hydrogen Bonding[1,2]

Dagmar Boenigk and Dietrich Mootz*

Contribution from the Institut für Anorganische Chemie und Strukturchemie, Universität Düsseldorf, D-4000 Düsseldorf, Federal Republic of Germany. *Received August 10, 1987*

Abstract: The formation of solid complexes at low temperatures in the system pyridine–hydrogen fluoride was studied by difference thermal analysis and X-ray powder diffraction. The melting diagram obtained reveals the existence of as many as eight intermediary compounds $C_5H_5N{\cdot}nHF$ with melting points between −1 and −124 °C and n assuming all integral values from one to eight. The crystal structures of four of these were determined from single-crystal Mo Kα diffractometer data: $C_5H_5N{\cdot}1HF$ (crystal system tetragonal, space group $P4_12_12$, $Z = 4$ formula units per unit cell), $C_5H_5N{\cdot}2HF$ (monoclinic, $P2_1/m$, $Z = 2$), $C_5H_5N{\cdot}3HF$ (triclinic, $P\bar{1}$, $Z = 2$), and $C_5H_5N{\cdot}4HF$ (monoclinic, $P2_1/m$, $Z = 2$). In the complex with $n = 1$ the base is not protonated by the acid and furnishes the first observation of the hydrogen bond F–H···N by crystal structure analysis. With an F···N distance of 247.2 (2) pm it is the strongest one known between a fluorine and a nitrogen atom. The remaining structures contain pyridinium cations and complex $H_{n-1}F_n^-$ anions and are governed by hydrogen bonding, too, between the cations and anions (N–H···F) as well as within the anions (F–H···F). Coulombic interaction appears to be largely internalized in discrete ionic pairs ($n = 2$ and 3) and a one-dimensional ribbon structure ($n = 4$).

The system pyridine–hydrogen fluoride is of practical importance in preparative organic chemistry. A solution in the pure base of about 70 wt % of anhydrous hydrogen fluoride (equivalent to 90 mol %) is described,[3] and in wide use, as a convenient reagent

0002-7863/88/1510-2135$01.50/0

Table I. Crystallographic Data and Some Numbers Related to the Structure Determinations

	$C_5H_5N \cdot 1HF$	$C_5H_5N \cdot 2HF$	$C_5H_5N \cdot 3HF$	$C_5H_5N \cdot 4HF$
mp, °C	−31 dec	−1	−17	−39
measuring temp, °C	−50	−110	−100	−104
crystal system	tetragonal	monoclinic	triclinic	monoclinic
space group; Z	$P4_12_12$; 4	$P2_1/m$; 2	$P\bar{1}$; 2	$P2_1/m$; 2
lattice constant				
a, pm	605.9 (8)	397.3 (4)	416.5 (2)	747.2 (1)
b, pm		792.1 (4)	736.4 (5)	689.49 (7)
c, pm	1428 (2)	937.1 (9)	1145.9 (5)	739.5 (1)
α, deg			82.31 (4)	
β, deg		92.97 (8)	87.78 (4)	100.08 (1)
γ, deg			77.16 (5)	
calcd density, g/cm^3	1.26	1.34	1.36	1.41
range of θ, deg	1.5–25	1.5–32.5	1.5–27.5	1.5–27.5
unique data: obsd; all	278; 315	867; 1007	1279; 1541	852; 928
parameters refined	46	60	114	83
R: obsd; all	0.028; 0.036	0.053; 0.059	0.051; 0.061	0.043; 0.046
R_w: obsd; all	0.038; 0.039	0.067; 0.068	0.069; 0.110	0.062; 0.062

for a variety of fluorination reactions. It is remarkably stable up to 55 °C, with the acid largely bound in anionic poly(hydrogen fluoride) species. The presence of these, and the concomitant pyridinium cations, in the solution was inferred from ^{19}F and ^1H NMR spectroscopy.[3]

The present work is a combined phase-analytical and structural study of the solid phases of the system existing at reduced temperatures. It was prompted by recent work in this laboratory on other binary (quasibinary) systems with the base (e.g., C_5H_5N–H_2O[4]) or the acid (e.g., HF–H_2O,[5] HF–NH_3[6]) as one of the components.

Experimental Section

Sample Preparation and Phase Analysis. Pyridine (99.5%, Baker Chemicals B. V.) was dried over potassium hydroxide, fractionated over a 1 m Vigreux column, and stored over molecular sieve. Hydrogen fluoride was freshly distilled from technical grade hydrofluoric acid (70–75%, Riedel-de Haen) in an all-PTFE apparatus. In a vacuum line with its parts out of the same material the two components were carefully mixed in varied proportions by slowly condensing the acid onto the base under cooling. Compositions of the storage solutions thus obtained were controlled by difference weighing and fluoride ion potentiometry. The samples for the subsequent experiments were either taken from these solutions themselves or prepared by mixing measured amounts of them and additional pyridine or hydrogen fluoride.

The formation of solid phases in the system was examined by working out its melting diagram over the entire concentration range and at temperatures between ca. −165 and 0 °C. The methods employed were difference thermal analysis (DTA) and temperature-dependent X-ray powder diffraction. For the DTA, samples of ca. 0.7 cm^3 were enclosed in PTFE ampules. Samples for the X-ray powder studies were sealed in PE tubings (0.5 mm inner diameter, 20–30 mm long), which were placed inside thin-walled glass capillaries for mechanical fixation. Details of the apparatus and techniques used are described and referred to elsewhere.[7]

Crystal Growth and Structure Determination. Four of the low-melting complexes of the system established by the phase analysis could be obtained in the form of single crystals suitable for X-ray structure determination. This was achieved on a Syntex $P2_1$ four-circle diffractometer equipped with a modified LT-1 low-temperature device. A miniature zone-melting technique using focused heat radiation[8] was applied while the samples, prepared in the same way as for the X-ray powder experiments, were kept in an adjustable gas stream at temperatures somewhat below their melting points.

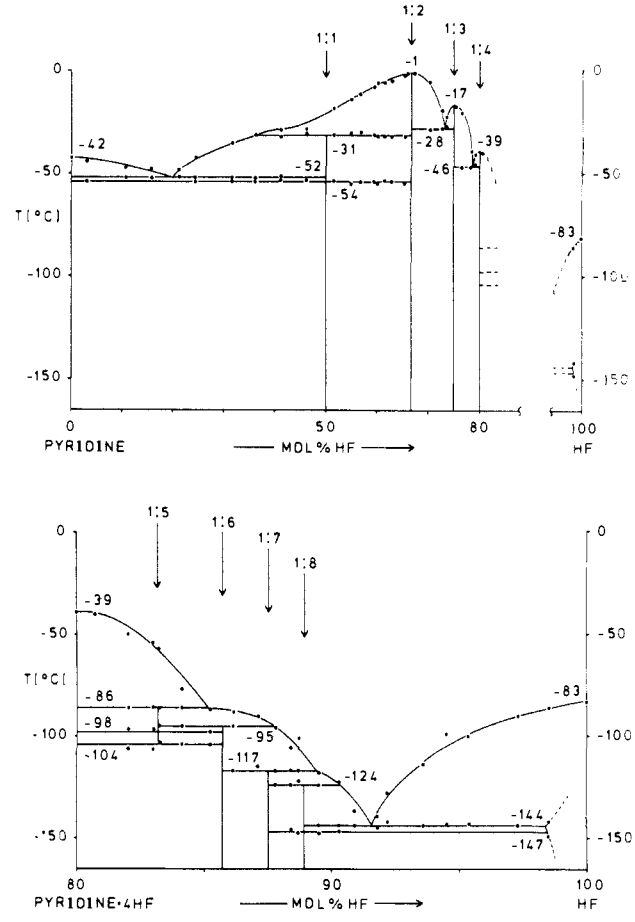

Figure 1. The melting diagram of the quasibinary system pyridine–hydrogen fluoride. The range 80–100 mol % HF is shown separately with an enlarged scale.

The X-ray measurements were done on the diffractometer with graphite-monochromatized Mo Kα radiation (λ = 71.073 pm, ω scan for intensities). Absorption errors were considered negligible and corrections not applied. The structures were solved by direct methods and refined by the method of least squares by using the observed reflections only ($|F_o| \geq 3.92\sigma_F$). The function minimized was $\sum w(|F_o| - |F_c|)^2$, with the weights $w = 1/(\sigma_F^2 + 0.0004|F_o|^2)$. The hydrogen atoms were located in difference maps of the electron density and refined isotropically. The compositions of the phases and some more experimental and computational details of the structure determinations are given in Table I.

The calculations were performed with the program system E-XTL (Syntex) and SHELXTL (Nicolet) on an Eclipse S/200 minicomputer

(1) Number 18 of the series Fluorides and Fluoro Acids. Number 17: Wiebcke, M.; Mootz, D. *Z. Kristallogr.*, in press.

(2) From the Dissertation of Boenigk, D. "Polyhydrogenfluoride: Stabilitätsbereiche und Kristallstrukturen"; Universität Düsseldorf, 1985.

(3) Olah, G. A.; Welch, J. T.; Vankar, Y. D.; Nojima, M.; Kerekes, I.; Olah, J. A. *J. Org. Chem.* **1979**, *44*, 3872–3881.

(4) Mootz, D.; Wussow, H.-G. *J. Chem. Phys.* **1981**, *75*, 1517–1522.

(5) Mootz, D.; Poll, W. *Z. Anorg. Allg. Chem.* **1982**, *484*, 158–164.

(6) Mootz, D.; Poll, W. *Z. Naturforsch., B* **1984**, *39B*, 290–297.

(7) Mootz, D.; Poll, W. *Z. Naturforsch., B* **1984**, *39B*, 1300–1305.

(8) Brodalla, D.; Mootz, D.; Boese, R.; Osswald, W. *J. Appl. Crystallogr.* **1985**, *18*, 316–319.

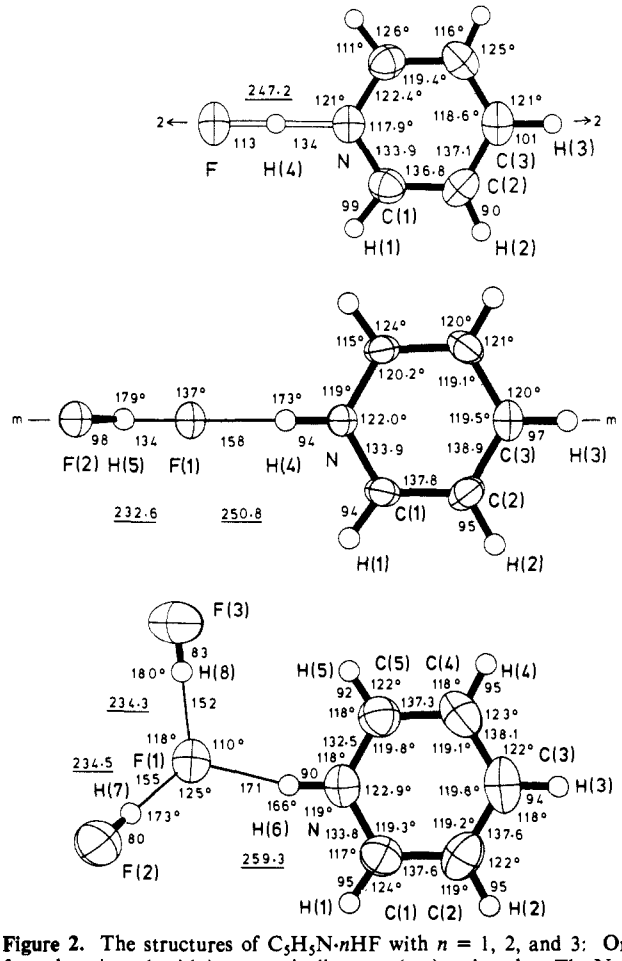

Figure 2. The structures of $C_5H_5N{\cdot}n$HF with n = 1, 2, and 3: One formula unit each with interatomic distances (pm) and angles. The N···F and F···F distances in the hydrogen bonds are underlined. The esd's are 0.1–0.3 pm and 0.1–0.2°, when hydrogen atoms are not involved, and otherwise 2–4 pm and 1–4°.

(Data General) and ORTEP II[9] on a TR 445 computer (Telefunken). In the drawings the atoms are represented by 50% probability ellipsoids, with the hydrogen atom thermal parameters uniformly reduced to 10^4 pm^2.

Results

The melting diagram obtained (Figure 1) shows the existence of as many as eight different solid compounds of pyridine and hydrogen fluoride at reduced temperatures. The compositions are $C_5H_5N{\cdot}n$HF with n assuming all integral values from one to eight. The complex with n = 1, 5, and 8 are dimorphic with a low- and a high-temperature form each, which increases the number of intermediary solid phases of the system to eleven. Details of their stability ranges and melting behavior can be read off the diagram directly. The highest and lowest melting points are at −1 and −124 °C and belong to the phases with n = 2 and 8, respectively.

The crystal structures determined are those of the phases $C_5H_5N{\cdot}n$HF with n = 1 (high-temperature form), 2, 3, and 4. The crystallographic data are listed in Table I and the atomic parameters in Table II. One formula unit each, with site symmetry 2, m, 1, and m, respectively, is depicted with interatomic distances and angles in Figures 2 and 3. The values are not corrected for thermal motion nor for the known systematic error of X-ray structure determination of shortening F–H (and N–H) bonds and consequently lengthening intermolecular H···F distances. Some additional structure detail for $C_5H_5N{\cdot}4$HF is given in Figure 3 also and in Table III. Stereoscopic drawings of larger parts of the crystal structures with their unit cells are assembled in Figure 4.

(9) Johnson, C. K. ORTEP II, ORNL-5138, Oak Ridge National Laboratory, Oak Ridge, TN 1976.

Table II. Atomic Parameters with Standard Deviations in Parentheses

	x	y	z	B^a
		$C_5H_5N{\cdot}1$HF		
N	0.0393 (3)	x	0.0	3.31 (4)
C(1)	0.0075 (3)	0.2323 (4)	0.0436 (1)	3.60 (5)
C(2)	0.1637 (4)	0.3952 (3)	0.0446 (1)	3.80 (5)
C(3)	0.3611 (4)	x	0.0	3.96 (5)
F	−0.2492 (2)	x	0.0	5.29 (4)
H(1)	−0.138 (4)	0.237 (4)	0.076 (1)	5.0 (5)
H(2)	0.128 (4)	0.518 (5)	0.076 (2)	5.4 (6)
H(3)	0.479 (5)	x	0.0	5.5 (8)
H(4)	−0.117 (8)	x	0.0	11 (1)
		$C_5H_5N{\cdot}2$HF		
N	0.2966 (3)	0.25	0.3755 (1)	2.37 (3)
C(1)	0.3720 (3)	0.1021 (1)	0.3157 (1)	2.61 (2)
C(2)	0.5338 (3)	0.0985 (2)	0.1892 (1)	2.90 (3)
C(3)	0.6156 (4)	0.25	0.1247 (2)	2.92 (4)
F(1)	−0.0436 (3)	0.25	0.5936 (1)	3.49 (3)
F(2)	0.0460 (3)	0.25	0.8408 (1)	3.47 (3)
H(1)	0.304 (4)	0.006 (2)	0.364 (2)	3.8 (4)
H(2)	0.596 (4)	−0.007 (2)	0.149 (2)	4.0 (4)
H(3)	0.747 (7)	0.25	0.040 (3)	4.5 (5)
H(4)	0.185 (6)	0.25	0.461 (3)	3.6 (5)
H(5)	0.005 (7)	0.25	0.736 (4)	6.9 (9)
		$C_5H_5N{\cdot}3$HF		
N	0.4233 (3)	0.6305 (2)	0.2331 (1)	3.54 (3)
C(1)	0.5531 (4)	0.7300 (3)	0.1447 (2)	4.06 (4)
C(2)	0.6461 (4)	0.8909 (2)	0.1650 (2)	4.55 (5)
C(3)	0.6063 (5)	0.9448 (3)	0.2760 (2)	4.89 (5)
C(4)	0.4750 (5)	0.8372 (3)	0.3653 (2)	5.01 (5)
C(5)	0.3838 (4)	0.6783 (2)	0.3410 (2)	4.07 (4)
F(1)	0.1488 (3)	0.3498 (1)	0.22225 (9)	4.73 (3)
F(2)	−0.0913 (4)	0.2744 (2)	0.0586 (1)	6.86 (5)
F(3)	−0.0617 (4)	0.2801 (2)	0.4115 (1)	6.73 (4)
H(1)	0.575 (5)	0.684 (3)	0.070 (2)	5.0 (5)
H(2)	0.745 (6)	0.959 (3)	0.103 (2)	5.7 (5)
H(3)	0.682 (7)	1.051 (4)	0.289 (2)	6.6 (6)
H(4)	0.426 (6)	0.874 (4)	0.441 (2)	6.3 (5)
H(5)	0.292 (5)	0.603 (3)	0.397 (2)	4.9 (4)
H(6)	0.347 (6)	0.531 (4)	0.218 (2)	5.7 (5)
H(7)	−0.024 (8)	0.305 (5)	0.116 (3)	7.9 (7)
H(8)	0.012 (7)	0.305 (4)	0.345 (3)	6.8 (7)
		$C_5H_5N{\cdot}4$HF		
N	0.2958 (2)	0.25	0.4662 (2)	2.76 (3)
C(1)	0.3998 (2)	0.25	0.6328 (2)	3.09 (4)
C(2)	0.3206 (2)	0.25	0.7868 (2)	3.18 (4)
C(3)	0.1337 (2)	0.25	0.7666 (2)	2.95 (4)
C(4)	0.0296 (2)	0.25	0.5917 (2)	2.90 (4)
C(5)	0.1141 (2)	0.25	0.4416 (2)	2.81 (4)
F(1)	0.6242 (2)	0.25	0.3348 (2)	4.51 (4)
F(2)	0.7593 (2)	0.25	0.0692 (1)	3.65 (3)
F(3)	0.7558 (1)	−0.0067 (1)	−0.1483 (1)	4.33 (3)
H(1)	0.526 (4)	0.25	0.636 (4)	4.2 (5)
H(2)	0.394 (5)	0.25	0.918 (5)	6.7 (8)
H(3)	0.083 (4)	0.25	0.871 (4)	3.9 (5)
H(4)	−0.097 (4)	0.25	0.575 (4)	3.8 (5)
H(5)	0.056 (4)	0.25	0.316 (4)	4.7 (6)
H(6)	0.345 (4)	0.25	0.371 (4)	4.3 (5)
H(7)	0.654 (5)	0.25	0.227 (5)	7.8 (9)
H(8)	0.750 (3)	0.085 (4)	−0.068 (3)	6.5 (5)

[a] The isotropic thermal parameters of the N, C, and F atoms were derived from the anisotropic B_{ij} values by $B = (1/3)(B_{11}a^2a^{*2} + B_{23}bcb^*c^* \cos\alpha + \ldots)$.

Table III. Some Additional Interatomic Distances and Angles of the Structure of $C_5H_5N{\cdot}4$HF (Esd's as in Figure 3)[a]

H(6)···F(1)	215 pm	N—H(6)···F(1)	133°
H(6)···F(3′)	238 pm	N—H(6)···F(3′)	116°
H(6)···F(1)—H(7)	122°	F(1)···H(6)···F(3′)	96°
H(6)···F(3′)—H(8′)	159°	F(3′)···H(6)···F(3″)	90°

[a] Prime: $1 - x, -y, -z$. Double prime: $1 - x, {}^1/_2 + y, -z$.

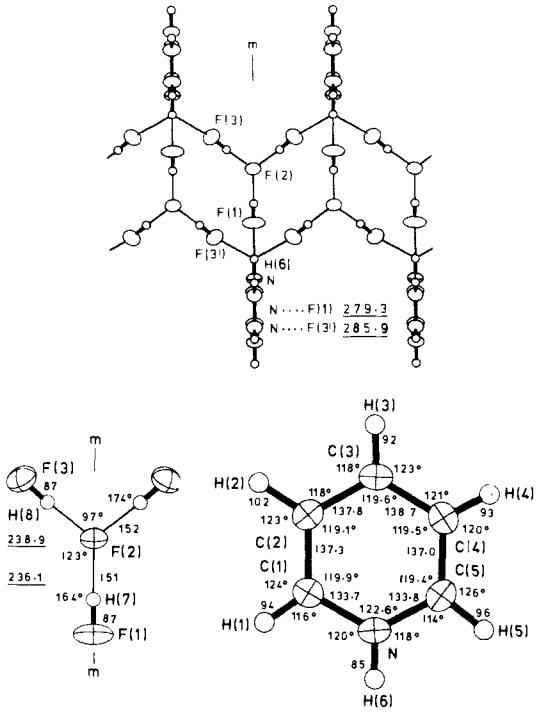

Figure 3. The structure of $C_5H_5N{\cdot}4HF$: A one-dimensional ribbon (above) and one formula unit with the ions shown separately (below). As for the rest, see Figure 2.

Discussion

The structures of the pyridine–hydrogen fluoride complexes determined are marked by very strong hydrogen bonding between the base and the acid and (or) within the acid component, where this is present in molar excess.

As a surprising feature of the comlex $C_5H_5N{\cdot}1HF$ the hydrogen atom in the NHF hydrogen bond is found distinctly closer to the fluorine than to the nitrogen atom, i.e., the base does not appear to be protonated by the acid. In line with this, the angle CNC at the nitrogen atom is the smallest of the bond angles in the aromatic ring, almost as small as in the crystal structures of the free base and its trihydrate,[4] while in each of the other complexes of this study, where protonation of the base does occur, it is the largest.

Hence, the hydrogen bond in the 1:1 complex is of the type F–H···N rather than N–H···F. It is actually the first hydrogen bond of this type and the shortest between a nitrogen and a fluorine atom established so far by crystal structure analysis. A case in point is the hydrogen bond F–H···O as opposed to O–H···F. It is also particularly short and rare, reported only in the crystal structures of $K[PHO_2(OH)]{\cdot}HF$[10] and $(C_6H_5)_3PO{\cdot}HF$.[11]

The complex $C_5H_5N{\cdot}2HF$, according to its crystal structure, can be reformulated as $C_5H_5NH^+HF_2^-$, pyridinium hydrogen difluoride. The hydrogen bond within the HF_2^- ion is almost as strong as that in the respective alkali metal salts, but it contains the hydrogen atom in a definitely off-centered position, close to the outer fluorine atom. The other hydrogen bond, between the nitrogen and the inner fluorine atom, is now of the type N–H···F and still very short. It binds the cation and anion in a discrete pair with the Coulombic interaction largely internalized. This description, which offers an explanation for the low melting point, has been suggested before, based on the low-temperature infrared spectrum, for the bonding in a related solid complex of hydrogen fluoride and the base trimethylamine.[12] Conclusions drawn from matrix infrared spectra, of hydrogen fluoride complexes of ammonia[13] and the methylamines,[14] present another interesting correspondence to the crystal structures of both the 1:1 and the 1:2 complex of this study.

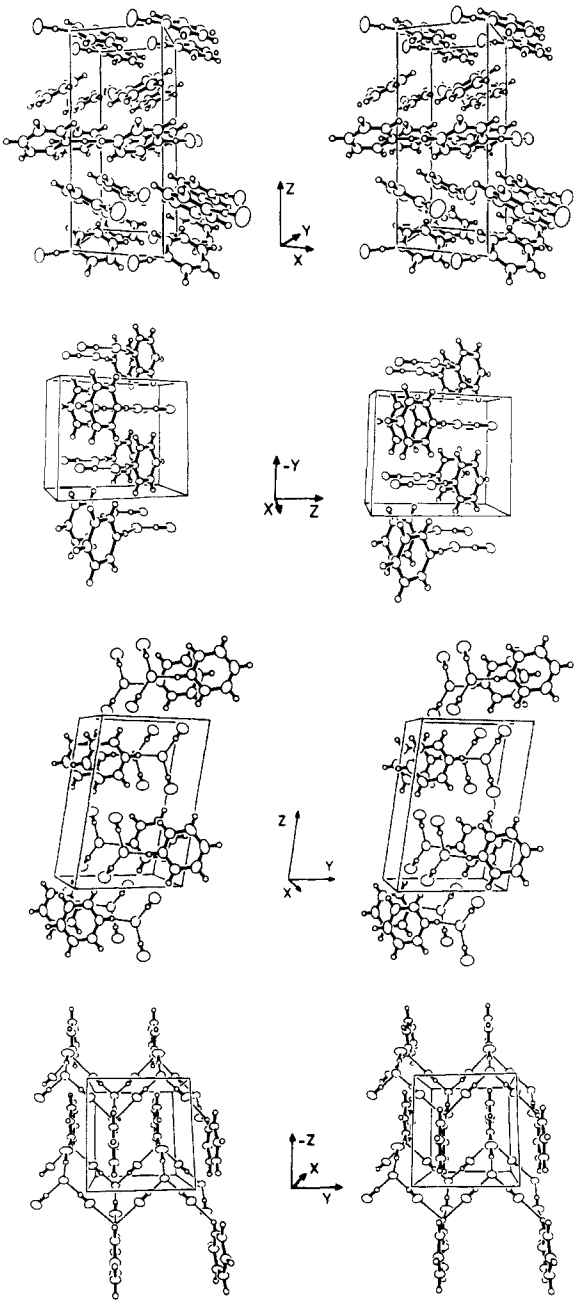

Figure 4. Stereoscopic drawings of larger parts of all four structures with n in $C_5H_5N{\cdot}nHF$ increasing from top to bottom.

Ionic formulae also hold for the crystal structures of the 1:3 and the 1:4 compound of pyridine and hydrogen fluoride, i.e., $C_5H_5NH^+H_2F_3^-$ and $C_5H_5NH^+H_3F_4^-$, respectively. But only in the 1:3 compound is the unit of structure again an internally neutralized, tightly bound zwitterionic molecular complex. In the crystal structure of the 1:4 compound, there are unlimited ribbons, along the b-axis direction, formed by trifurcated hydrogen bonds $N–H(\cdots F)_3$ between the cation and three anions, and vice versa. Both the angular $H_2F_3^-$ and the distorted trigonal-pyramidal $H_3F_4^-$ ions, with increasingly larger average hydrogen bonding F···F distances, have been characterized in several crystal structures

(10) Altenburg, H.; Mootz, D. *Acta Crystallogr. B* **1971**, *B27*, 1982–1986.
(11) Thierbach, D.; Huber, F. *Z. Anorg. Allg. Chem.* **1979**, *451*, 137–142.
(12) Gennick, I.; Harmon, K. M.; Potvin, M. M. *Inorg. Chem.* **1977**, *16*, 2033–2040.
(13) Johnson, G. L.; Andrews, L. *J. Am. Chem. Soc.* **1982**, *104*, 3043–3047.
(14) Andrews, L.; Davis, S. R.; Johnson, G. L. *J. Phys. Chem.* **1986**, *90*, 4273–4282.

before, most recently in those of the respective tetramethylammonium salts.[15]

Crystal structure determinations of the remaining complexes of the system, with 5 to 8 mol of hydrogen fluoride per mol of pyridine, will most probably reveal these as pyridinium poly(hydrogen fluorides), too. Anions $H_4F_5^-$ and, in one instance each, $H_5F_6^-$ and $H_7F_8^-$ are already established species in the solid state.[6,15]

(15) Mootz, D.; Boenigk, D. *Z. Anorg. Allg. Chem.* **1987**, *544*, 159-166.

Acknowledgment. This work was supported by the Minister für Wissenschaft und Forschung des Landes Nordrhein-Westfalen and by the Fonds der Chemischen Industrie.

Registry No. C_5H_5N, 110-86-1; HF, 7664-39-3; $C_5H_5N \cdot 1HF$, 32001-55-1; $C_5H_5N \cdot 2HF$, 87979-78-0; $C_5H_5N \cdot 3HF$, 79162-49-5; $C_5H_5N \cdot 4HF$, 85351-48-0.

Supplementary Material Available: Listing of anisotropic thermal parameters for the non-hydrogen atoms (2 pages); structure factor tables (8 pages). Ordering information is given on any current masthead page.

Kinetics, Mechanisms, and Catalysis of Oxygen Atom Transfer Reactions of *S*-Oxide and Pyridine *N*-Oxide Substrates with Molybdenum(IV,VI) Complexes: Relevance to Molybdoenzymes

John P. Caradonna,[1a] P. Rabindra Reddy,[1b] and R. H. Holm*

Contribution from the Department of Chemistry, Harvard University, Cambridge, Massachusetts 02138. *Received August 10, 1987*

Abstract: The kinetics and mechanism of the oxygen atom transfer reactions $MoO_2(L\text{-}NS_2) + (R_F)_3P \rightarrow MoO(L\text{-}NS_2)(DMF) + (R_F)_3PO$ (1) and $MoO(L\text{-}NS_2)(DMF) + XO \rightarrow MoO_2(L\text{-}NS_2) + X$, with X = $(R_F)_2SO$ (2) and 3-fluoropyridine *N*-oxide (3), have been investigated in DMF solutions (L-NS_2 = 2,6-bis(2,2-diphenyl-2-mercaptoethyl)pyridine(2-), R_F = *p*-C_6H_4F). The following rate constants (297.5 K) and activation parameters were obtained: reaction 1, k_2 = 9.7 (4) × 10^{-3} M^{-1} s^{-1}, $\Delta H^{\ddagger}$ = 11.7 (6) kcal/mol, $\Delta S^{\ddagger}$ = -28.4 (1.6) eu; reaction 2, k_1 = 14.0 (7) × 10^{-4} s^{-1}, $\Delta H^{\ddagger}$ = 22.1 (1.3) kcal/mol, $\Delta S^{\ddagger}$ = 2.6 (1.6) eu; reaction 3, k_1 = 16.0 (8) × 10^{-4} s^{-1}, $\Delta H^{\ddagger}$ = 23.4 (1.4) kcal/mol, $\Delta S^{\ddagger}$ = 7.2 (2.0) eu. Reactions 2 and 3 exhibit saturation kinetics, under which the rate-determining step is intramolecular atom transfer. Mechanisms and transition states are proposed. The activation parameters are the first measured for oxo transfer from substrate; the small activation entropies suggest a transition state structurally similar to the complex $MoO(L\text{-}NS_2)(XO)$ formed in a labile equilibrium prior to oxo transfer to Mo. Coupling of reaction 1 with reaction 2 or 3 affords the catalytic reaction 4, $(R_F)_3P + XO \rightarrow (R_F)_3PO + X$; no reaction occurs in the absence of the Mo catalyst. The kinetics of catalysis were examined by monitoring the concentrations of reactants and products by ^{19}F NMR spectroscopy. After 15 h, each system showed ca. 100 turnovers. Reaction 4 with XO = $(R_F)_2SO$ has a catalytic rate constant of 7 × 10^{-3} M^{-1} s^{-1}, close to the value for reaction 1. This and other considerations show that the catalytic rate is limited by the rate of oxo transfer from the Mo(VI) complex $MoO_2(L\text{-}NS_2)$. An attempt to establish the catalytic mechanism led to detection of inhibition; the inhibitory species could not be identified. These results provide the most detailed information on the kinetics and mechanisms of Mo-mediated oxygen atom transfer and demonstrate the efficacy of ^{19}F NMR for detecting and monitoring catalysis and determining catalytic velocities and rate constants. The relation of these results to the enzymatic reduction of *N*-oxides and *S*-oxides is briefly discussed.

In this laboratory we have developed analogue reaction systems[2-5] for molybdoenzymes that catalyze the addition or removal of an oxygen atom from generalized substrate X/XO. These enzymes are usually referred to as hydroxylases; their properties have been reviewed in some detail.[6-10] Our working hypothesis is that at least some of these enzymes catalyze substrate oxidation or reduction by the forward or reverse reaction 1, in which an

$$Mo^{VI}O_2L_n + X \rightleftharpoons Mo^{IV}OL_n + XO \qquad (1)$$

oxygen atom is directly transferred to or removed from substrate without obligatory intervention of any other reactant. In this case, we denote the enzymes as oxo-transferases. A system that has proven to be extremely useful is that of reaction 2, which effects stoichiometric reduction of a number of substrates, including *S*-oxides, *N*-oxides, and nitrate, and also stoichiometric oxidation of tertiary phosphines.

The design of analogue reaction systems, with particular attention to requisite properties of the complexes that serve as representations of the Mo-containing catalytic sites, has been considered elsewhere.[3,11,12] Briefly, complexes $MoO_2(L\text{-}NS_2)$ and $MoO(L\text{-}NS_2)(DMF)$ contain coordination units not inconsistent

(1) (a) National Institutes of Health Postdoctoral Fellow, 1985-1987. (b) Overseas Associate, 1986-1988, Department of Biotechnology, Government of India; on leave from the Department of Chemistry, Osmania University, Hyderabad 500007, India.
(2) Berg, J. M.; Holm, R. H. *J. Am. Chem. Soc.* **1984**, *106*, 3035.
(3) Berg, J. M.; Holm, R. H. *J. Am. Chem. Soc.* **1985**, *107*, 925.
(4) Harlan, E. W.; Berg, J. M.; Holm, R. H. *J. Am. Chem. Soc.* **1986**, *108*, 6992.
(5) Caradonna, J. P.; Harlan, E. W.; Holm, R. H. *J. Am. Chem. Soc.* **1986**, *108*, 7856.
(6) Bray, R. C. In *The Enzymes*; Boyer, P. D., Ed.; Academic: New York, 1975; Vol. XII, Part B, Chapter 6.
(7) Bray, R. C. *Adv. Enzymol. Relat. Areas Mol. Biol.* **1980**, *51*, 107.
(8) Coughlan, M. P., Ed. *Molybdenum and Molybdenum-Containing Enzymes*; Pergamon: New York, 1980.
(9) Spiro, T. G., Ed. *Molybdenum Enzymes*; Wiley-Interscience: New York, 1985.
(10) Holm, R. H. *Chem. Rev.* **1987**, *87*, 1401.
(11) Holm, R. H.; Berg, J. M. *Pure Appl. Chem.* **1984**, *56*, 1645.
(12) Holm, R. H.; Berg, J. M. *Acc. Chem. Res.* **1986**, *19*, 363.

0002-7863/88/1510-2139$01.50/0